Boundary and current elements for simulation of electromagnetic fields of complicated spatial configuration

***†A.A. Trubitsyn, E. Yu. Grachev and V.S. Gurov**

Department of Electronics, Ryazan State Radio Engineering University, Russia

*Presenting and †corresponding author: assur@bk.ru

Abstract

Processes of interaction of charged particle fluxes with substance are a base of operation of a wide range of devices for scientific researches and vacuum technological installations for various purposes. Besides, an important independent scientific and technical task is a task to control parameters of such fluxes by influencing of electrical and/or magnetic fields of a specified configuration on them.

The paper shows a mathematical instrument and algorithms for simulation of the electrical field in electron-optical systems with complicated configuration of electrodes by the boundary element method (BEM). The boundary element method solves an exterior Dirichlet's problem under digitization of a multiplied connected boundary of the area by straight boundary elements. Integral equation being a basic for the method is found from the second Green's formula.

Biot-Savart-Laplace law is used for numerical simulation of the magnetic field for a set of arbitrarily oriented round solenoids. Besides, each turn of the solenoid is divided into current elements having a physically short extent. Calculation of the magnetic field of a two-dimensional shape (turn) in space is reduced to calculation of coordinates of elementary current middles and their projections on the axes $0x$ and $0y$. Magnetic field of a solenoid is calculated as a superposition of fields of all its turns. Magnetic field of the arbitrarily oriented solenoid can be found by means of direct and reverse rotations of the Cartesian coordinate system for angles being equal to angles setting an orientation of solenoids in space. Magnetic field of a set of arbitrarily oriented solenoids is calculated according to the superposition principle.

Developed methods have been integrated into the computer application and used under design of the microfocus x-ray tube of high power. Acceleration and focusing of the electron beam in the tube is executed by the electrostatic field and its positioning to the required area on the anode – by the magnetic field of two external solenoids.

Keywords: boundary elements, boundary elements method, electron optics system, Biot-Savart-Laplace law, current element, solenoid, numerical modelling, microfocus x-ray tube

Introduction

Tasks of focusing and transportation of charged particle fluxes are main problems under creation of highly qualitative devices for electron and ion optics. Electric and magnetic fields and their combinations are used for solution of such tasks. Mathematical simulation is one of important stages for development of technical means forming electromagnetic fields with required properties. Numerical methods are the most general techniques for simulation of electromagnetic fields as distinct from analytical ones.

Electrostatic field simulation

The problem of numerical analysis of electric fields in systems with a complex configuration of electrodes is brought to the forefront in electron optics which is the basis for analytical instrument making [1] [2]. At present Boundary Elements Method is one of the most advanced numerical techniques to solve problems of the potential theory [3]. The solution of the exterior Dirichlet problem in electron optics, in contrast to the interior one, allows us to predict the parameters of the schemes as close to the real device.

In this case boundary Γ of the researched area G is represented by a combination of closed contours (electrodes of real thickness and configuration) at each of which potential is fixed and integral equation connecting potential $u(\xi)$ in the researched area and its boundary with a normal potential derivative q at the boundary is recorded. The obtained integral relations are based on the second Green's identity [4] that allows simulating fields in areas which boundaries have corners and fractures.

A wide class of electron-optical systems (EOS) can be described within the framework of axi-symmetrical models at the design stage with a high degree of confidence.

For numerical solution of the problem the integral equation has a discrete form. For this purpose boundary Γ is divided into N boundary elements Γ_j. Taking into consideration potential constancy at each contour (electrode) and under assumption of the normal potential derivative constancy at each boundary element, the equation is recorded in the form

$$\gamma u(\xi)+\sum_{j=1}^{N} u_j H_j(\xi)=\sum_{j=1}^{N} q_j F_j(\xi), \qquad (1)$$

where $\xi \in G \cup \Gamma$; $\gamma=\pi$ under $\xi\in\Gamma$ and $\gamma=2\pi$ under $\xi\in G$ for two-dimensional tasks, $\gamma=2\pi$ under $\xi\in\Gamma$ and $\gamma=4\pi$ under $\xi\in G$ for three-dimensional tasks, and functions $F_j(\xi)$ and $H_j(\xi)$ are integrals from the fundamental solution and from a normal derivative of the fundamental solution of the Laplace equation correspondingly [5] and in a regular case they can be calculated according to the standard Gaussian quadrature.

Calculation of the electrostatic field is executed by two stages. Firstly, by means of equation (1) an unknown vector q_j is calculated according to a known boundary distribution of the potential u ($\xi\in\Gamma$), i.e. "inverse" problem is solved. Then found values q_j and specified u_j for determination of the function $u(\xi)$, $\xi\in\Omega$ from equation (1) are used, i.e. "direct" problem is solved.

Copyright technique [6] is briefly described below for elimination and weakening of peculiarities in sub-integral functions (integrands) under solution of inverse and direct problems providing high accuracy of the task solution in general.

Inverse problem

Collocation method is used for solution of the inverse problem according to which points ξ_i are determined in the middle of each *straight* (then $\gamma(\xi)=2\pi$) element Γ_i and for the whole N- aggregate of points ξ_I a system of N equations is recorded

$$2\pi u(\xi_i)+\sum_{j=1}^{N} u_j H_{ij}=\sum_{j=1}^{N} q_j F_{ij}, \; i=1, 2, \ldots ,N, \qquad (2)$$

where $H_{ij}=H_j(\xi_i)$,$F_{ij}=F_j(\xi_i)$.

Integrals with singular integrands exist under $i=j$, i.e. in the case when integration is executed by element Γ_j (let's call it as singular) containing a current collocation point ξ_i.

Calculation of H_{ii}. In consequence of potential jump of a double layer under crossing of the area boundary inside-out [7] we will have the following value of integral H_{ii} for the exterior task:

$$H_{ii}=4\pi.$$

Calculation of F_{ii}. In this case for elimination of peculiarities, polynomial representation of the complete elliptical integral of I-type is used

$$K(m)=B(m_1)-A(m_1)\ln m_1, \text{ where } m_1=1-m,\ B(m_1)=\sum_{n=0}^{N_K} p_n m_1^n,\ A(m_1)=\sum_{n=0}^{N_K} s_n m_1^n,$$

p_n, s_n - tabulated coefficients of the polynomial representation [8] which ensures enough high speed of convergence to an exact value and allows obtaining the following estimation of integral F_{ii}

$$F_{ii}=4\Delta\chi_i\left\{\int_0^1\Big[G_0(\xi_i,x)+\ln 2\Big(G_i(-x)+G_i(x)\Big)\Big]dx+\int_0^1\Big(G_i(-x)+G_i(x)\Big)\ln(1/x)dx\right\}, \qquad (3)$$

where $G_0(\xi_i,x)=\left[\left(B(m_1)+A(m_1)\ln\dfrac{a^*+b^*}{\Delta\chi_i^2}\right)R(x)/\sqrt{a^*+b^*}\right]$,

$a^*+b^*=[R(\xi)+R(x)]^2+[Z(\xi)-Z(x)]^2$, $R(x)=c_ix+d_i$, $Z(x)=a_ix+b_i$,

$$B(m_1)=\sum_{n=0}^{N_k} p_n m_1^n=\sum_{n=0}^{N_k} p_n\left[\frac{(\xi_i-x)^2\Delta\chi_i^2}{a^*+b^*}\right]^n,\quad A(m_1)=\sum_{n=0}^{N_k} s_n m_1^n=\sum_{n=0}^{N_k} s_n\left[\frac{(\xi_i-x)^2\Delta\chi_i^2}{a^*+b^*}\right]^n,$$

$$G_i(x)=\left\{\big((1+x)c_i+2d_i\big)\frac{\sum_{n=0}^{N_k} s_n\left(\dfrac{(x\Delta\chi_i)^2}{[c_i(2+x)+4d_i]^2+(xa_i)^2}\right)^n}{\sqrt{[c_i(2+x)+4d_i]^2+(xa_i)^2}}\right\},$$

$\Delta\chi_j$ - a length of straight boundary element Γ_j, $c_i=\sin(\phi)\Delta\chi_i$, $a_i=\cos(\phi)\Delta\chi_i$, b_i and d_i are z- and r-coordinates of the element Γ_i beginning in the cylindrical coordinate system $Z0R$, ϕ - an angle of its slope to the axis z.

The first integral in formula (3) can be calculated by means of the usual Gaussian quadrature and there are special quadratures [8] allowing making calculations with required accuracy for numerical integration of functions of type $f(x)\ln(1/x)$. Multiplicative approach has methodologically been realized here for separation of peculiarities.

So, solution q_j of the inverse problem according to (2) can be obtained from a system of linear equations

$$b_i=F_{ij}q_j,$$

where $b_i=\sum_{j=1}^{N} H_{ij}^* u_j$, $i,j=1,2,\ \dots,N$; $H_{ij}^*=H_{ij}$ for $i\neq j$; $H_{ii}^*=2\pi+H_{ii}=6\pi$; F_{ij} is calculated according to formula (3) for $i=j$.

Direct problem

Obvious formula is used for solution of the direct problem (ref. equation (1))

$$u(\xi)=\frac{1}{4\pi}\left[\sum_{j=1}^{N}u_j H_j(\xi)-\sum_{j=1}^{N}q_j F_j(\xi)\right],\ \xi\in\Omega.$$

It is clear that the closer point ξ is to the boundary element Γ_j,, the stronger extremum expression is in behavior of integrands (discontinuity occurs at the limit) that complicates direct application of the standard Gaussian quadrature.

Formulas improving accuracy of estimation of (quasi-) singular integrals $H_j(\xi)$ and $F_j(\xi)$ are mentioned below.

For accurate estimation of integral $H_j(\xi)$ the following formula is used

$$H_j(\xi)=H_j^*(\xi)-P(\xi)/(r_j)^k,$$

where an unknown parameter $P(\xi)$ is determined by expression

$$P(\xi)=\frac{\sum_{j=1}^{N}H_j^*}{\sum_{j=1}^{N}(r_j)^{-k}}.$$

Here $H_j^*(\xi)$ are integrals calculated according to the standard Gaussian quadrature, r_j is a distance between ξ and a point being the closest to it in the segment Γ_j, k is an index of the degree which empirically found optimal value is equal to 4.

Formula for calculation of $F_j(\xi)$:

$$F_j(\xi)=4\Delta\chi_j\left\{\begin{array}{l}\int_0^1\left[\frac{K(m)}{\sqrt{a^*+b^*}}R(x)+g(D/T)\ln(Tx^2-2Dx+P)\right]dx-\\ -g(D/T)\left[\begin{array}{l}(1-D/T)\ln(T-2D+P)+D\ln(P)/T-2+\\ +2\frac{\sqrt{TP-D^2}}{T}\left(arctg\frac{D}{\sqrt{TP-D^2}}+arctg\frac{T-D}{\sqrt{TP-D^2}}\right)\end{array}\right]\end{array}\right\}.$$

Here $g(x)=A(m_1)R(x)/\sqrt{a^*+b^*}$, $T=\Delta\chi_j$, $D=[R(\xi)-d_j]c_j+[Z(\xi)-b_j]a_j$, $P=[R(\xi)-d_j]^2+[Z(\xi)-b_j]^2$.

Additive approach for separation of peculiarities has methodologically been realized here.

Calculation error estimate

Testing of suggested methods for solution of the exterior Dirichlet's problem on model axially symmetrical tasks has allowed making the following conclusions:

- guaranteed accuracy of the potential calculation is ~ 10^{-4}-10^{-3} %;
- for electron-optical systems (EOS) with straight sections of electrodes, calculation errors in the range are limited only by round-off errors.
- for EOS with curvilinear electrodes, calculation errors are determined by an accuracy of approximation of the boundary by linear segments and do not exceed ~ 10^{-3} % under calculation in real time.

Figure 1, as an example, shows a result of simulation of the electrostatic field in the microfocus x-ray tube containing a cathode assembly which elements are under potential -80 kV, focusing electrode with potential -78 kV and grounded thick anode with a narrow channel of the special form intended for increasing of power of x-ray radiation. Distribution of the potential is encoded by shades of grey color.

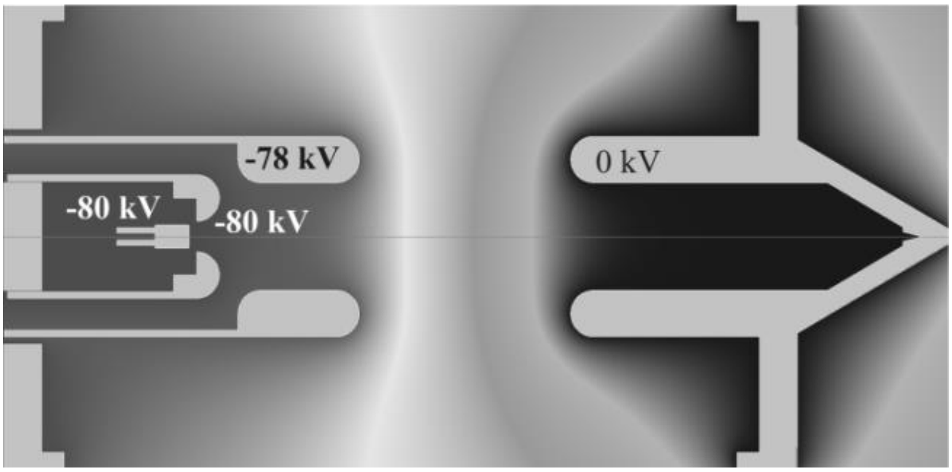

Figure 1. Distribution of an electrical potential in the x-ray tube meridional section

Magnetic field simulation

Known method for the magnetic field excitation in space is based on transmission of the electrical current through conductors. Biot-Savart-Laplace law [9] is one of main laws of electromagnetism and sets a value of the magnetic field induction $d\vec{B}$ created in space by a current element $Id\vec{l}$ according to formula

$$d\vec{B} = \frac{Id\vec{l}\times\vec{r}}{r^3(x_0,y_0,z_0,x,y,z)},$$

where I is a value of current in the element $d\vec{l}(x_0, y_0, z_0)$ of the contour (l), $\vec{r}$ is a distance between element $d\vec{l}$ and point of observation $P(x,y,z)$ (Fig. 2). Here $I=I_{SI}\cdot 10^{-7}$, where I_{SI} – current measured in amperes. The superposition principle allows calculating a magnetic field at any point of space $P(x,y,z)$ by integrating according to contour (l):

$$\vec{B} = \int_{(l)} d\vec{B} = \int_{(l)} \frac{Id\vec{l}\times\vec{r}}{r^3(x_0,y_0,z_0,x,y,z)}. \quad (4)$$

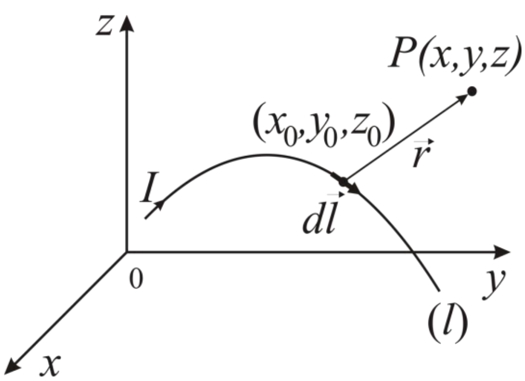

Figure 2. Calculation of the magnetic field at point *P*

One of main sources of the magnetic field in the absence of ferromagnetic is a solenoid as a combination of simple circular currents. However, direct application of the Biot-Savart-Laplace law even for calculation of the field of a circular turn (at any point of space) is complicated by problems with analytical integration in formula (4).

Then a simple method of numerical solution of the task to calculate a field of the circular turn is mentioned and obtained results are generalized for technique of determination of an arbitrary solenoid field.

Field of circular current

Idea of the suggested method is the following. Flat conductor located in the plane $x0y$ is divided into N similar segments of length Δl (Fig. 3). Distance r is considered as constant under integration by one element Δl_i and equal to a distance between a midpoint of the segment with coordinates (x_i,y_i,z_i) and a point P.

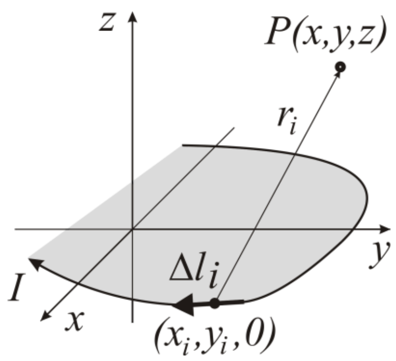

Figure 3. Numerical determination of the flat current magnetic field

In such approximation integral (4) is recorded in the following way:

$$\vec{B} \approx I \sum_{i=1}^{N} \int_{(\Delta l_i)} \frac{d\vec{l} \times \vec{r}_i}{r_i^3} \approx I \sum_{i=1}^{N} \frac{1}{r_i^3} \int_{(\Delta l_i)} d\vec{l} \times \vec{r}_i. \qquad (5)$$

Then we take into account that $d\vec{l} = d\vec{l}(dx, dy, 0)$ and $\vec{r}_i = \vec{r}_i(x - x_i, y - y_i, z)$, and also a vector product is recorded though determinant

$$d\vec{l} \times \vec{r}_i = \begin{vmatrix} \vec{i} & \vec{j} & \vec{k} \\ dx & dy & 0 \\ x - x_i & y - y_i & z \end{vmatrix} =$$

$$= z dy \vec{i} - z dx \vec{j} + [(y - y_i)dx - (x - x_i)dy]\vec{k}.$$

Taking this record into consideration integral over the segment Δl_i is easily expressed by

$$\int_{(\Delta l_i)} d\vec{l} \times \vec{r}_i = z\Delta y_i \vec{i} - z\Delta x_i \vec{j} + [(y - y_i)\Delta x_i - (x - x_i)\Delta y_i]\vec{k}. \qquad 6)$$

Since in the coordinate form a vector of the magnetic induction is recorded in the following way $\vec{B} = B_x\vec{i} + B_y\vec{j} + B_z\vec{k}$, then on the basis of formulas (5) and (6) we obtain an expression for components of the vector $\vec{B}$ along coordinate axes

$$B_x = I \sum_{i=1}^{N} \frac{z\Delta y_i}{r_i^3},\ B_y = -I \sum_{i=1}^{N} \frac{z\Delta x_i}{r_i^3},\ B_z = I \sum_{i=1}^{N} \frac{(y-y_i)\Delta x_i - (x-x_i)\Delta y_i}{r_i^3}, \qquad (7)$$

where distance r_i has an obvious expression

$$r_i = \sqrt{(x - x_i)^2 + (y - y_i)^2 + z^2}.$$

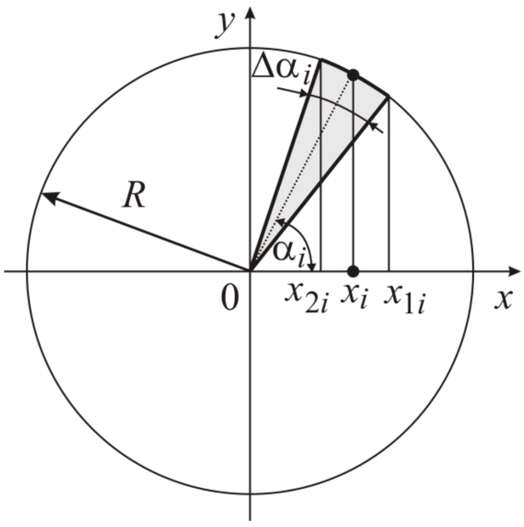

Figure 4. Division of the circular contour into current elements

So, calculation of the magnetic field created by the flat contour with current is reduced to calculation of coordinates x_i, y_i of element middles Δl_i, $i=1 \ldots N$, and projections Δx_i, Δy_i of these elements along axes $0x$ and $0y$.

For a circular turn with current located perpendicularly to the axis $0z$ with a center at the beginning of coordinates, enough simple algorithm for calculation of these parameters consists in division of the circumference (Fig. 4) into the same arcs with a small angular size $\Delta\alpha$ and determination of an angular coordinate of the element center

$$\alpha_i = (i - 1)\Delta\alpha + \frac{\Delta\alpha}{2},\ i=1, 2, \ldots, N,$$

determination of coordinates of its center

$$x_i = Rcos\alpha_i,\, y_i = Rsin\alpha_i \tag{8}$$

and values of projections of the element along axes 0x and 0y

$$\Delta x_i = x_{2i} - x_{1i},\, \Delta y_i = y_{2i} - y_{1i} \tag{9}$$

where $x_{1i} = Rcos[(i-1)\Delta\alpha]$, $x_{2i} = Rcos(i\Delta\alpha)$, $y_{1i} = Rsin[(i-1)\Delta\alpha]$, $y_{2i} = Rsin(i\Delta\alpha)$.

Solenoid field

Suggested technique for calculation of the turn field easily spreads to a problem of calculation of the solenoid magnetic field containing K layers and J turns in each layer (Fig. 5).

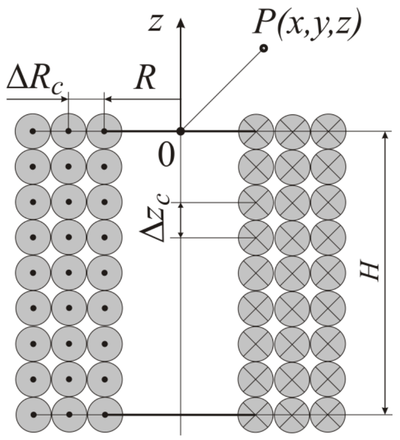

Figure 5. Solenoid cross-section

Solenoid field which upper base is located in the plane $x0y$ and axis coincides with coordinate axis 0z can be calculated as a double sum by a number of layers and turns in each layer

$$\vec{B}_S(x,y,z) = \sum_{k=1}^{K}\sum_{j=1}^{J}\vec{B}_{kj}\left(x,y,z_j(z)\right), \tag{10}$$

where components of the magnetic field $\vec{B}_{kj}$ of each turn along axes are determined according to formula (7) taking into account a value of the turn radius of κ-layer $R_k=R+(k-1)\Delta R_c$ for usage in formulas (8, 9), $k=1...K$, and $z_j=z+(j-1)\Delta z_c$, $j=1...J$. Here ΔR_c is a difference of radiuses of turns and Δz_c is a distance between adjacent turns along axis 0z.

Calculation error estimate

Analytical expression for the field of the circular current on the symmetry axis

$$B_0 = \frac{I}{2}\frac{R^2}{(R^2+z^2)^{3/2}},$$

where z – a distance from the turn center to a calculated point, allows testing the suggested technique for numerical determination of the magnetic induction.

Fig. 6 shows a dependence of a value of the relative error of induction calculation $B=B_z$ (7) in the turn center (z=0) from a number N of elements of division of the rolling circumference.

Fig. 7 shows a dependence of the absolute error of the magnetic field induction calculation $\Delta B = |B_0 - B_z|$ on the turn axis with current I=1 arb. u. and radius R=1 arb. u. for N=180, so, we can make a conclusion on enough fast attenuation of the error with distance from the turn plane.

Errors of the magnetic field calculations in solenoids have been estimated by the same way. For a solenoid with internal radius R=1 and length H=10 containing 5 layers of turns and 1000 turns in each layer under division of the turn circumference into N=360 elements, relative error of the field calculation was 0.1 % in the solenoid center.

Analysis of above mentioned data allows making a conclusion that the suggested method ensures high accuracy of calculations of the magnetic field being enough for correct solution of tasks of contemporary electron optics.

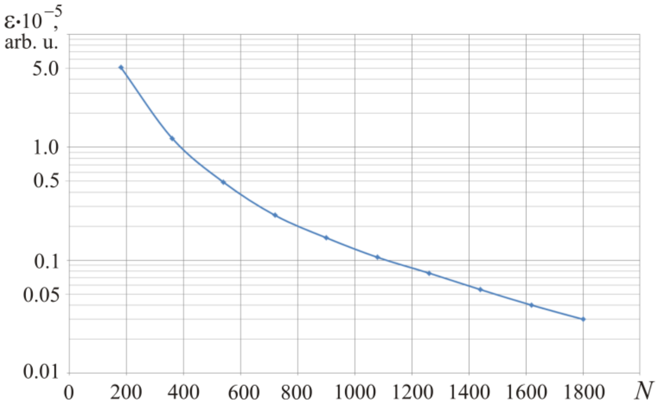

Figure 6. Relative error of the magnetic field calculation at the circular current center

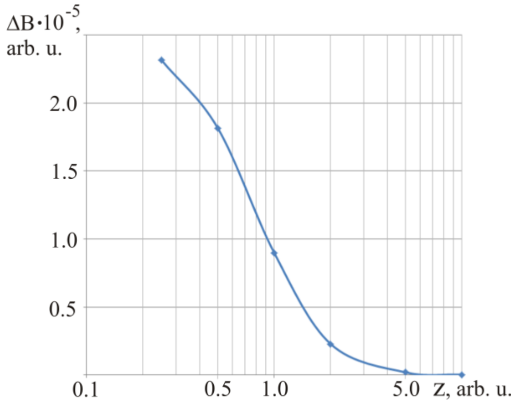

Figure 7. Absolute error of the magnetic field calculation on the circular current axis

Field of the arbitrarily oriented solenoid

Location of the solenoid in space can be definitely set by coordinates x_S, y_S and z_S of the upper base center and angles α and β fixing direction of its axis. Direction of the axial field vector $\vec{B}$ determined according to the right-hand screw rule (Fig. 8) in relation to the current direction is accepted as a positive direction of the solenoid axis $\vec{S}$. Angles α and β are angles of solenoid axis rotation around axes $0x'$ and $0y'$ in the coordinate system $0x'y'z'$ connected with the upper base center which all axes are codirected with axes of the laboratory coordinate system $0xyz$.

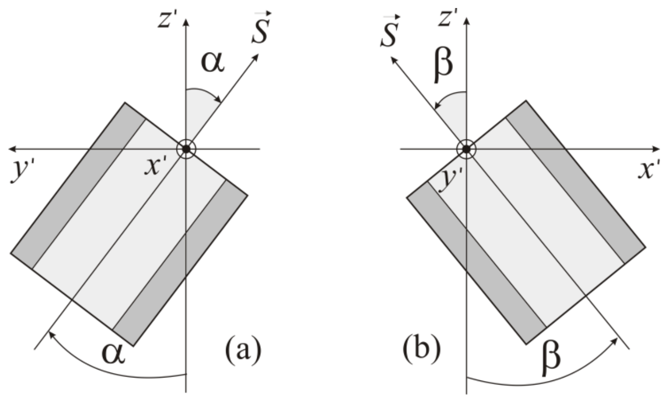

Figure 8. Location of the solenoid in space determined by angles of rotation α and β of its axis $\vec{S}$ around coordinate axes $0x'$ and $0y'$

Under specified center coordinates x_S, y_S, z_S in the coordinate system $0xyz$ and angles of orientation α and β of the solenoid, at the first stage the algorithm for calculation of the magnetic field induction $\vec{B}_S$ at the point (x,y,z) consists in a sequential usage of standard formulas for transformation of coordinates under rotations and application of formula (10) in the following way

$$\vec{B}_{SR}(x,y,z) = \vec{B}_S(x_\beta, y_\beta, z_\beta),$$

where $x_\beta = x_\alpha \cos\beta + z_\alpha \sin\beta$, $y_\beta = y_\alpha$, $z_\beta = z_\alpha \cos\beta - x_\alpha \sin\beta$.

Here $x_\alpha = x - x_S$, $y_\alpha = (y - y_S)\cos\alpha + (z - z_S)\sin\alpha$, $z_\alpha = (z - z_S)\cos\alpha - (y - y_S)\sin\alpha$.

At the second stage for final estimation of magnetic induction components $\vec{B}_S(x,y,z) = B_{Sx}\vec{\imath} + B_{Sy}\vec{\jmath} + B_{Sz}\vec{k}$ inverse rotations of the vector $\vec{B}_{SR} = B_{SRx}\vec{\imath} + B_{SRy}\vec{\jmath} + B_{SRz}\vec{k}$ should be executed according to expressions:

$$B_{x\alpha} = B_{SRx},\ B_{y\alpha} = B_{SRy}\cos\alpha - B_{SRz}\sin\alpha,\ B_{z\alpha} = B_{SRz}\cos\alpha + B_{SRy}\sin\alpha,$$

$$B_{Sx} = B_{x\alpha}\cos\beta - B_{z\alpha}\sin\beta,\ B_{Sy} = B_{y\alpha},\ B_{Sz} = B_{z\alpha}\cos\beta + B_{x\alpha}\sin\beta.$$

Field of a set of arbitrarily oriented solenoids

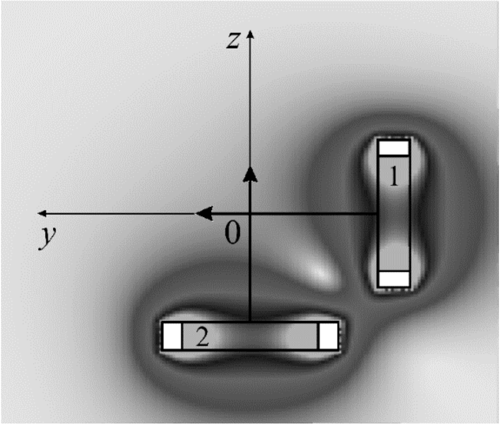

Figure 9. Map of a magnitude of the magnetic induction of two solenoids

It is obvious that in the case of several solenoids calculation of the magnetic field $\vec{B}$ is executed by summation of components of induction $\vec{B}_S$ or in a short form

$$\vec{B}(x, y, z) = \sum_S \vec{B}_S(x, y, z).$$

Fig. 9 shows results of simulation of the magnetic field of two solenoids (1 and 2) with orthogonally related axes. Relation of the exterior diameter to the interior one of each solenoid is 4:3. Distribution of the field is represented in the plane passing through axes of solenoids and encoded by shades of grey color.

Design of the microfocus x-ray tube

At present there is enough rapid expansion of microfocus x-ray tube applications. It caused by the fact that microfocus sources of x-ray radiation have a range of advantages in comparison with macrofocus ones:

• microfocus sources are essentially able to ensure high locality of researches;

• microfocus instruments ensure a higher quality of images under equal doses in the receiver plane;

• microfocus sources allow obtaining increased (in 5-10 times) images.

From the point of view of electron optics, microfocus x-ray source (tube) is an axially-symmetrical electron-beam generator. Traditionally electron generators are made in the form of a sequence of the cathode modulator assembly, several lens systems for acceleration and focusing and, if necessary, an electron-optical circuit for electron beam sweeps in raster on the target surface.

Microfocus tubes of the transmission type ensure the best quality of images. However, power of such tubes with a planar anode cannot exceed 10-20 W due to strong local heating of the anode surface. One of methods to increase power of tubes of transmission type consists in execution of a narrow channel with special form in the thick anode [10]. Under bombardment by accelerated electrons wall of the channel become sources of x-ray quanta.

Above mentioned methods for calculation of electrical and magnetic fields have been integrated in the copyright software FOCUS [11] intended for simulation of electron-optical systems of the wide range. Example of the trajectory analysis of an x-ray microfocus tube with axially-symmetrical construction is shown in Fig. 10. A narrow channel is executed in the anode. Symmetry axis is indicated as $0x$. Distribution of the electrical field in a tube is shown in Fig. 1.

Exact positioning of the electron beam into the channel can be ensured by the system of magnetic deviation consisting, for example, of two solenoids (ref. Fig. 9) which axes are perpendicularly to the symmetry axis $0x$. Simulation of the tube with two solenoids 1 and 2 installed outside has shown a possibility of electron beam positioning at any point of the anode surface. So, under the current value 100 ampere-turns in any of solenoids, a value of the trajectory deviation Δr on the anode from the axis $0x$ is approximately 10% of the solenoid exterior radius (Fig. 11).

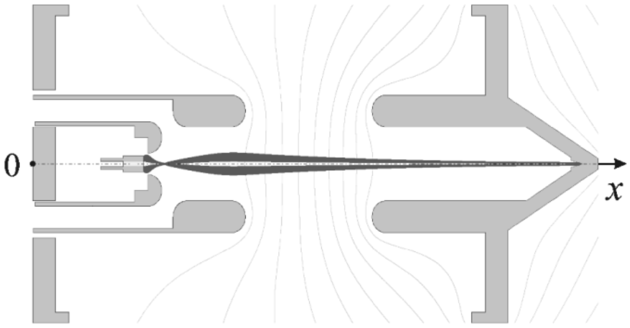

Figure 10. Electron-optical scheme of the microfocus x-ray tube

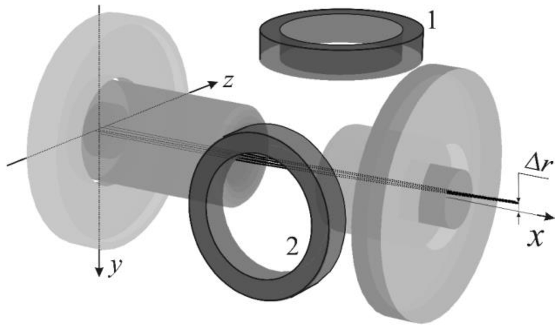

Figure 11. Deviation of the electron beam by the solenoid magnetic field

Conclusions

Boundary Elements Method for simulation of electrostatic fields in axially-symmetrical electron-optical systems with practically arbitrary configuration of electrodes has been developed.

Current Elements Method for simulation of magnetic fields of a set of solenoids arbitrarily oriented in space has been suggested and researched.

Methods for simulation of fields have been integrated into the copyright software FOCUS intended for design of a system with electromagnetic fields of complicated special configuration.

Results of simulation of a microfocus x-ray tube with high power have been represented.

Acknowledgments

The research has been carried out at expenses of the Russian Scientific Fund grant (project No.15-19-00132).

References

[1] Golikov, Yu. K. and Krasnova, N. K. (1999) Electrostatic mass spectrometer for concurrent mass-, energy- and angle-resolved measurements, *Nucl Instrum Meth Phys Res A* **427** (1-2), 208-212.

[2] Cubric, D., De Fanis, A., Konishi and I., Kumashiro, S. (2011) Parallel acquisition electrostatic electron energy analyzers for high throughput nano-analysis, *Nucl Instrum Meth Phys Res A* **645** (1), 227-233.

[3] Cheng, Alexander H.-D. and Cheng, Daisy T. (2005) Heritage and early history of the boundary element method, *Engineering Analysis with Boundary Elements* **29** (3), 268–302.

[4] Greenberg, M. D. (1971*). Application of Green's functions in science and engineering*. Englewood Cliffs, Prentice Hall, NJ, USA.

[5] Brebbia, C. A. , Telles, J. C. F. and Wrobel, L. C. (2012) *Boundary Element Techniques: Theory and Applications in Engineering*, Springer, London, UK.

[6] Gurov, V.S., Saulebekov, A.O. and Trubitsyn A.A. (2015) *Analytical, Approximate-Analytical and Numerical Methods in the Design of Energy Analyzers*, In P.W. Hawkes (Ed.), Advances in Imaging and Electron Physics **192**, Academic Press, London, UK.

[7] Courant, R. and Hilbert, D. (1989) *Methods of mathematical physics*, Interscience Publishers, New York, USA.

[8] Abramovitz, M. and Stegun, I. A. (Eds.), (1964). *Handbook of mathematical functions*, National Bureau of Standards, Gaithersburg, MD, USA.

[9] Griffiths, D. (1998) *Introduction to Electrodynamics*, Addison-Wesley Professional, Prentice Hall, NJ, USA.

[10] Trubitsyn, A.A., Grachev, E.Yu. and Dubkov, M.V. (2016) *A microfocus X-ray Tube with High Power*, Proceedings of the 15th International Seminar ”Recent Trends in Charged Particle Optics and Surface Physics Instrumentation”. Skalský dvur near Brno, Czech Republic.

[11] http://www.focuspro-soft.com.